Transverse load sensing based on a dual-frequency optoelectronic oscillator

Fanqi Kong, Wangzhe Li, and Jianping Yao*

Microwave Photonics Research Laboratory, School of Electrical Engineering and Computer Science, University of Ottawa, Ontario K1N 6N5, Canada

**Corresponding author: jpyao@eecs.uottawa.ca*

Received April 8, 2013; revised June 20, 2013; accepted June 20, 2013; posted June 25, 2013 (Doc. ID 188456); published July 15, 2013

We propose and experimentally demonstrate a fiber-optic sensor implemented based on a dual-frequency optoelectronic oscillator (OEO) for transverse load sensing. In the OEO loop, a phase-shifted fiber Bragg grating (PS-FBG) is employed to which a transverse load is applied to introduce a birefringence to create two orthogonally polarized notches, which leads to the generation of two oscillating frequencies. The beat frequency between the two oscillating frequencies is a function of the load force applied to the PS-FBG. The proposed sensor is experimentally demonstrated. The sensitivity and the minimal detectable load are measured to be as high as ~9.73 GHz/(N/mm) and 2.06×10^{-4} N/mm, respectively. The high-frequency purity and stability of the generated microwave signal by the OEO permit extremely reliable and high-accuracy measurement. The frequency interrogation allows the system to operate at an ultra-high speed. In addition, the sensing signal is insensitive to the variations of both the environmental temperature and the optical carrier wavelength.

OCIS codes: (060.2370) Fiber optics sensors; (230.4910) Oscillators.

http://dx.doi.org/10.1364/OL.38.002611

In past decades fiber Bragg grating (FBG) sensors that have numerous applications, such as structural health monitoring [1,2], medical treatment [3], and pipeline security monitoring [4] have been widely investigated. The unique features of an FBG sensor include ultra-high sensitivity, compactness, and multiplexing capability. The immunity to electro-magnetic interference makes an FBG sensor particularly suitable for applications where the environmental conditions are harsh. Among various physical quantities, an FBG-based sensor can measure the transverse load, a vital parameter in structural health monitoring, and is measurable through the nonaxisymmetric load induced birefringence in a fiber. Conventionally, however, the bandwidth of a uniform FBG is much broader than the birefringence induced frequency shift, which severely limits the sensing sensitivity and resolution. For this reason, a π phase-shifted FBG (PS-FBG), which has a narrow notch (~10 MHz) in its reflection window, has been employed as a sensor probe [5–7]. When a load force is applied to the PS-FBG, it becomes birefringent, and the narrow reflection notch will be split into two, with the spacing in between having a direct relationship with the applied load. However, conventional schemes based on wavelength interrogation using an optical spectrum analyzer are rather slow and the resolution is also limited. Thanks to the high speed and high resolution of an electrical spectrum analyzing technique, frequency interrogation in the electrical domain has been proposed to solve such a problem [6–10]. The sensing information is converted from the optical domain to the electrical domain, which can be directly detected by an electronic spectrum analyzer (ESA). A dual-wavelength laser-based configuration is commonly used, though the stability and signal quality are far from satisfactory [6–11].

In this Letter, we propose a novel approach to realizing frequency interrogation of a PS-FBG-based transverse load sensor, which is implemented by incorporating the PS-FBG into a dual-frequency optoelectronic oscillator (OEO). The high-frequency purity and stability of the generated RF signal by the OEO permit very reliable and high-accuracy measurement [12].

Figure 1 shows the configuration of the proposed transverse load sensor based on a dual-frequency OEO incorporating a PS-FBG. An optical carrier from a laser source is sent to a polarization modulator (PolM) via a polarization controller. The PolM is a special phase modulator that supports phase modulation along the orthogonal principal axes with opposite modulation indices. For simplicity, here we assume that the incident light is aligned with one of the principal axis of the PolM and thus the PolM is operating as a phase modulator. The phase-modulated signal is then sent to the PS-FBG through an optical circulator. One sideband of the phase-modulated signal is removed by the notch of the PS-FBG, and the phase-modulated signal is converted to a single-sideband intensity-modulated (SSB-IM) signal and is detected at a photodetector (PD). The detected electrical signal is sent back to the PolM after amplification by an electrical amplifier to close the OEO loop. Mathematically, the electrical field at the output of the PolM is given by

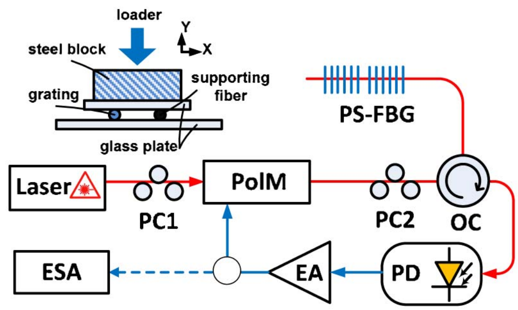

Fig. 1. Configuration of the proposed transverse load sensor. PolM, polarization modulator; PC, polarization controller; PD, photodetector; EA, electrical amplifier; ESA, electrical spectrum analyzer; PS-FBG, phase-shifted fiber Bragg grating; OC, optical circulator.

$$\begin{aligned} E_{\mathrm{PM}}(t) &= E_0 \exp\{j[\omega_c t + \pi(V_e/V_\pi)\cos(\omega_{\mathrm{RF}}t)]\} \\ &\approx E_0\{J_0(\beta)e^{j\omega_c t} + J_1(\beta)e^{j(\omega_c-\omega_{\mathrm{RF}})t+\pi/2} \\ &\quad - J_1(\beta)e^{j(\omega_c-\omega_{\mathrm{RF}})t-\pi/2}\}, \end{aligned} \tag{1}$$

where ω_c is the frequency of the optical carrier, V_e is the voltage applied to the PolM, V_π is the half-wave voltage of the PolM, and ω_{RF} is the frequency of the RF signal. If we directly detect the phase-modulated signal at the PD, due to the π -phase difference between the $+1$st and -1st order sidebands, the beating between optical carrier and the $+1$st order sideband will completely cancel the beating between optical carrier and the -1st order sideband. However, when the phase-modulated signal is directed to the PS-FBG, one sideband will be filtered out by the notch of the PS-FBG and a SSB-IM signal is generated. The detection of the SSB-IM signal at the PD will generate a RF signal [13,14]. The RF signal is amplified, and then sent back to the PolM to close the OEO loop. Thus, an oscillation signal with a frequency corresponding to the spacing between the wavelengths of the optical carrier and the sideband is generated.

If a transverse force is applied to the PS-FBG, the PS-FBG will be birefringent, the notch will then be split into two notches due to different refractive indices along the orthogonal directions. The frequency spacing between the two notches along the two orthogonal polarization states is given by [10]:

$$\Delta\nu = \nu_x - \nu_y = cB/n_0\lambda_0, \tag{2}$$

where B is the load-induced birefringence, given by

$$B = 2n_0^3(p_{11} - p_{12})(1 + \nu_p)\cos(2\theta)F/\pi rE, \tag{3}$$

where p_{11} and p_{12} are the components of the strain-optical tensor of the optical material, v_p is Poisson's ratio, E is the Young's modulus of the fiber, r is the radius of the fiber, θ is the angle between the direction of the force and the polarization axis of the fiber, and F is the linear transverse load (force per unit length).

Due to the load-interrelated notches along the orthogonal polarization directions, two RF signals at different frequencies are generated by the OEO. The beating between the two RF signals will generate a third microwave signal with its frequency being a function of the load-induced birefringence. Thus, by measuring the beat frequency, the transverse load applied to the PS-FBG can be measured.

A proof of concept experiment is performed. A PS-FBG written in a polarization maintaining fiber is fabricated. Because of the intrinsic birefringence, two notches with an initial notch separation of ~6 GHz are produced. The 3 dB bandwidth of each of the notches is ~30 MHz, which is narrow enough to ensure only a single longitudinal mode oscillation inside the OEO loop for each polarization state.

When a linearly polarized incident light with an angle of 45° relative to one principal axis of the PolM is sent to the PolM, the light is equally projected to the two orthogonal polarization axes, thus a photonic microwave filter having dual passbands with a band separation of 6 GHz is generated. Figure 2(a) shows the passband of the filter along the horizontal or vertical polarization direction, measured by aligning the incident light having an angle of 0° or 90° relative to one principal axis of the PolM. Figure 2(b) shows the filter response when the incident light is aligned with an angle of 45° relative to one principal axis of the PolM. A dual pass band filter is realized. When the OEO loop is closed, two microwave signals at two frequencies determined by center frequencies of the two passbands will be generated.

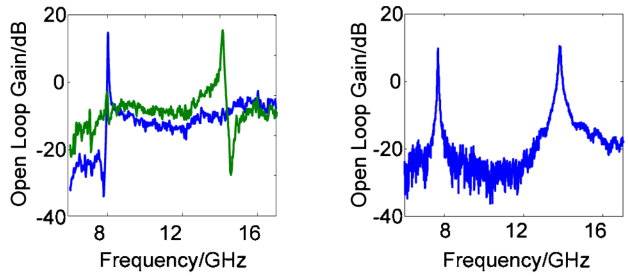

Fig. 2. (a) Single passband photonic microwave filter when the incident light is alighted with an angle of 0° or 90° relative to one principal axis of the PolM. (b) Dual passband photonic microwave filter when the incident light is alighted with an angle of 45° relative to one principal axis of the PolM.

Note that due to the nonlinearity of the PolM, a third signal that is the beat note of the two microwave signals is also generated. The frequency of the beat note is directly associated with the birefringence introduced by the transverse load to the PS-FBG. Thus, by measuring the beat frequency, the transverse load is measured.

By using the typical values of a silica fiber at a wavelength of 1550 nm[7], $n_0 = 1.444$, $p_{11} = 0.12$, $p_{12} = 0.27$, $v_p = 0.17$, $E = 7.6 \times 10^4\ \mathrm{N/mm^2}$, and the radius of optical fiber $r = 62.5\ \mu\mathrm{m}$, we have the relationship between the transverse load the beat frequency given by $d\nu/dF \approx 9.6\ \mathrm{GHz/(N/mm)}$.

Due to the intrinsic birefringence of the PS-FBG, two microwave signals at 8.22 and 14.24 GHz and a corresponding beat note at 6.02 GHz are generated, as shown in Fig. 3. To ensure the system reaches to its highest sensitivity and to have a good linearity between the transverse load and the beat frequency, in the experiment the transverse load is applied to the PS-FBG along the fast axis. Note that a supporting fiber with an identical radius is placed in parallel with the PS-FBG to ensure

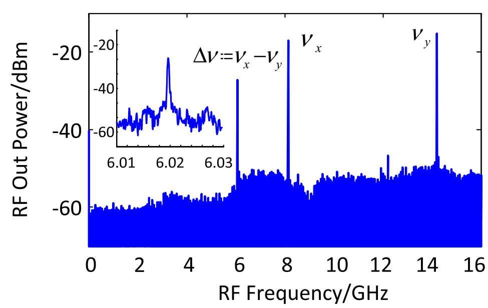

Fig. 3. Electrical spectrum of the signal generated by the dual-frequency OEO, with two microwave signals at 8.22 and 14.24 GHz and a beat signal at 6.02 GHz. Inset: the zoom-in view of the beat signal.

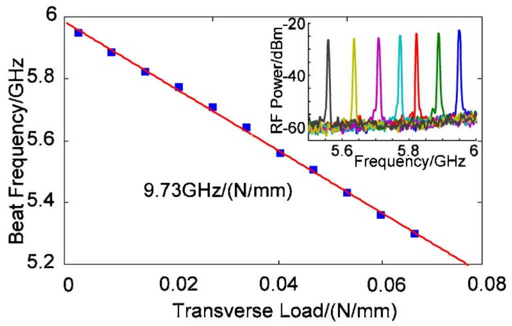

Fig. 4. Measured beating frequency as a function of applied transverse load and the electrical spectrum with different load. Inset: the electrical spectrum with different load.

the load is transversely applied. By increasing the load applied to the PS-FBG, the beat frequency is shifted linearly toward a smaller frequency, as shown in Fig. 4. The spectrum of the beat signal is measured by an ESA (Agilent E4448A), with the spectrum shown in the inset of Fig. 4. The slope through linear fitting is −9.73 GHz/(N/mm) which agrees well with the theoretical value of 9.6 GHz/(N/mm).

The stability of the sensor system is then studied. To do so, we let the system to operate in a room environment for two hours. The variation of the beating frequency is within 1 MHz. The resolution of the proposed sensor system is also studied. The resolution is limited by its free spectral range (FSR). In this system the FSR is calculated to be about 2 MHz, which corresponds to a resolution of 2.06×10^{-4} N/mm. The bandwidth of each of the notches of the PS-FBG is about 30 MHz, which is greater than the FSR of the loop of 2 MHz. The single mode operation of the OEO is ensured by properly controlling the loop gain.

We should note that the accuracy of the sensor is not affected by the wavelength drift of the laser source since the impact of wavelength drift is eliminated by the simultaneous shifting of the two oscillating frequencies. This property is important and can reduce significantly the system cost since no precise control of the wavelength of the laser source is needed.

The impact of the temperature change to the measurement is also studied. Although the birefringence of the fiber will be affected by temperature variation, such effect is much less significant than the birefringence induced by the geometrical asymmetry due to the transverse load [5,7]. It is demonstrated that the change in the beat frequency is within 2 MHz when the temperature is increased from 28°C to 48°C.

In the experiment, the PS-FBG is fabricated using a polarization maintaining fiber, which ensures an initial birefringence, leading to a nonzero beat frequency at ~6 GHz. The PS-FBG can be replaced by a regular PS-FBG written in a single-mode fiber without an initial birefringence. Thus, the beating frequency can be lower. The benefits of a system operating at a low interrogation frequency are obvious; the interrogation system can be implemented using lower frequency components at a lower cost.

In conclusion, we have proposed and experimentally demonstrated a transverse load fibre-optic sensor based on an OEO incorporating a PS-FBG with high resolution and fast-speed interrogation. The fundamental concept of the work was the use of an OEO incorporating a PS-FBG, to which a transverse load was applied, to translate the force applied to the PS-FBG to the change of the beat frequency. Since the interrogation is performed in the electrical domain, the system is simplified with an increased interrogation speed and accuracy. The proposed system was experimentally demonstrated. The sensitivity was measured to be as high as ~9.73 GHz/(N/mm). The stability of the system and the independence of the system on the environmental temperature change and the wavelength drift were also studied.

The work was supported by the Natural Sciences and Engineering Research Council of Canada.

References

1. M. Jones, Nat. Photonics **2**, 153 (2008).
2. H. Guo, G. Xiao, N. Mrad, and J. P. Yao, Sensors **11**, 3687 (2011).
3. E. Pinet, Nat. Photonics **2**, 150 (2008).
4. H. Nakstad and J. T. Kringlebotn, Nat. Photonics **2**, 147 (2008).
5. M. LeBlanc, S. T. Vohra, T. E. Tsai, and E. J. Friebele, Opt. Lett. **24**, 1091 (1999).
6. H. Fu, X. Shu, C. B. Mou, L. Zhang, S. He, and I. Bennion, IEEE Photon. Technol. Lett. **21**, 987 (2009).
7. J. T. Kringlebotn, W. H. Loh, and R. I. Laming, Opt. Lett. **21**, 1869 (1996).
8. Y. Zhang, B. O. Guan, and H. Y. Tam, Opt. Commun. **281**, 4619 (2008).
9. L. Gao, L. Chen, L. Huang, S. Liu, Z. Yin, and X. Chen, IEEE Sensor J. **12**, 1513 (2012).
10. B. O. Guan, L. Jin, Y. Zhang, and H. Y. Tam, J. Lightwave Technol. **30**, 1097 (2012).
11. J. Zhang, Q. Sun, R. Liang, J. Wo, D. Liu, and P. Shum, Opt. Lett. **37**, 2925 (2012).
12. M. Li, W. Li, J. P. Yao, and J. Azana, in *Advanced Photonics Congress*, OSA Technical Digest (online) (Optical Society of America, 2012), paper BTu2E.3.
13. W. Li, M. Li, and J. P. Yao, IEEE Trans. Microwave Theor. Tech. **60**, 1287 (2012).
14. W. Li and J. P. Yao, IEEE Trans. Microwave Theor. Tech. **60**, 1735 (2012).